J Mol Model (2013) 19:919–930
DOI 10.1007/s00894-012-1642-6

ORIGINAL PAPER

Global and local reactivity indexes applied to understand the chemistry of graphene oxide and doped graphene

Diego Cortés Arriagada

Received: 13 June 2012 / Accepted: 7 October 2012 / Published online: 21 October 2012
© Springer-Verlag Berlin Heidelberg 2012

Abstract At the density functional theory level, the electronic reactivity of oxidized and doped (with N, B, and P) graphene (G) has been analyzed. Molecular hardness and electrophilicity were used as global reactivity descriptors, while those at the local level, Fukui functions, Mulliken charges and molecular electrostatic potential were used in the order to characterize the intramolecular and intermolecular reactivity. These descriptors show that in GO, the global and local reactivity of the basal plane is improved mainly by hydroxyl groups, which improve besides the physisorption of small molecules, while, the active carbon atoms around the functional group would allow enhancement of the consecutively chemisorption. Furthermore, epoxide, carbonyl and carboxyl groups allow mainly enhancement of intermolecular non-covalent interactions. On the other hand, doping with N and B atoms increases the electrophilic character and the reactivity in the bulk. Specifically, in N-doped G, N and around carbon atoms would be able to serve as active sites of detection by frontier-controlled processes, explaining the improvement in electrochemical sensing; in addition, electron-deficient carbon atoms around N enhance the physisorption. Respecting the B-doped G, dopant and carbon atoms adjacent to B act as donor sites, suggesting that adsorption of cations on B-doped G is a frontier-controlled process; moreover, positively-charged B atoms enhance charge-controlled interactions with polarized molecules, and consecutively, in a frontier-controlled step, chemisorption is possible. Finally, P-doping increases the electrophilic reactivity in the bulk; also, P atoms enhance the physisorption of chemical species with negatively-charged centers or lone-pair electrons, and consecutively, chemisorption on P is possible.

Keywords Conceptual DFT · Doped graphene · Functionalized graphene · Graphene · Graphene oxide

D. Cortés Arriagada (✉)
Facultad de Química y Biología,
Universidad de Santiago de Chile,
Avenida Libertador Bernardo O'Higgins 3363. Estación Central,
Santiago, Chile
e-mail: diego.cortesa@usach.cl

Introduction

Graphene (G) has emerged quickly in material science as one of the most promising candidates to become the material of the future, being broadly studied by experimental and theoretical science. G is a semi-metal with a high electronic mobility (larger than 200,000 $cm^2 \cdot V^{-1} \cdot s^{-1}$) [1, 2], high thermal conductivity (>4000$W \cdot m \cdot K^{-1}$) [3], and its larger tensile strength makes it the strongest material ever measured [4]. In addition, by means of Raman spectroscopy, it has been shown that the reactivity of G monolayers is 10 times larger than in bi or multilayer of G, indicating that the 2-dimensional character has an effect in the chemical properties [5].

Based on the rising information, researchers began to synthesize new hybrid materials based in G, studying changes on the surface that tunes its physical and chemical properties. The graphene oxide (GO) has been used as a good alternative to synthesize nanomaterials of G, with the advantage that is a low-cost precursor; GO is a G lattice rich in oxygen containing functional groups (epoxide, hydroxyl, carboxyl, and carbonyl) [6, 7], which can be obtained from the graphite oxide through Hummers' method [8]. The functional groups in GO significantly increase its chemical reactivity and solubility, allowing the synthesis of hybrid materials or nanocomposites with potentials applications in optoelectronics [9, 10], catalysis [11–13], and electrochemistry [14, 15].

In addition, the chemical doping of G monolayers has also been used to both improve its chemical properties [16–20] and adjust its electrical character from semi-metal to semi-conductor [21]. The adsorption properties of G toward gases and amino acids are improved by means of the chemical doping [18, 19], enhancing specificity; this has potential application in the development of electrochemical sensors. Besides, N and B-doped G have shown the lithium and hydrogen adsorption enhancement, for applications in lithium ion batteries [21, 22] and storage in fuel cells [23], respectively.

The reactivity of G has been experimentally studied by spectroscopic analysis, showing that the reactivity on edges of G monolayers is twice larger than in its bulk [5]. Computationally, the inert reactivity of the basal plane of G has also been determined by Hernandez et al. by conceptual DFT using Fukui functions [24], finding that the most susceptible sites for electrophilic interactions are located on the periphery; these results agree with the one determined by Peralta et al. using average local ionization energy [25], and with the theoretical-thermodynamic studies developed by Radovic [26]. Structural modifications of G by functionalization or doping allow improvement of G reactivity, as noted before; these changes are mainly caused by inclusions of donor and acceptor groups (or atoms) that enhance the coulomb or charge-controlled interactions. For example, in GO, hydroxyl and epoxide groups become more negatively charged than G, enhancing interaction with metal cluster [27]; in addition, due to the larger electronegativity of oxygen atoms in the functional groups with respect to carbon atoms, these serve as the site for the physisorption by hydrogen bonds of polar molecules as H_2O and NH_3 [28]. On the other hand, in doped G, different effects can be observed according to the nature of the dopant: theoretical calculations done by Gong et al. [29] on N-doped G show an increment in the atomic charge of the carbons adjacent to the doping atoms, which suggest a considerable increase in the local reactivity of these atoms. In B-doped G, the insertion of an atom with five electrons turns G into an electron-deficient system [23, 30–32], causing an increase in its global electrophilic character, being more significant with the increase in the number of dopant atoms. Also, at DFT level, Garcia et al. show that P-doping increase the electrophilic character in the atoms located near to impurities [33].

In this computational study, the electronic structure of functionalized and doped G has been studied, focusing in its electronic reactivity with respect to pristine G. In order to understand the changes on global and local reactivity of G systems, conceptual-DFT derived descriptors, population analysis and molecular electrostatic potential have been used. Moreover, the obtained results are used to explain and analyze some experimental and theoretical facts related to the use and application of G systems.

Theory

In the DFT context, the derivatives of the energy $E\left[N, v\left(\vec{r}\right)\right]$ with respect to the number of electrons N and the external potential $v\left(\vec{r}\right)$ generate a set of properties that allow to characterize the global and local reactivity of the molecular systems from its electronic structure [34]. At global level, molecular hardness η denotes the disposition of the system to distort its electronic density [35], and in this sense, we must understand that η is a descriptor that indicates how reactive a molecular system is. By means of the Koopman's theorem, η is obtained as:

$$\eta = \left[\frac{\partial^2 E}{\partial N^2}\right]_{v\left(\vec{r}\right)} \approx \varepsilon_{LUMO} - \varepsilon_{HOMO} \tag{1}$$

ε_{LUMO} and ε_{HOMO} correspond to the energy of the lowest unoccupied (LUMO) and highest occupied molecular orbital (HOMO), respectively. On the other hand, electrophilicity ω is an index that characterizes the electrophilic character, defined as the stability in energy that reaches the molecular system when it gains electrons [36, 37]. ω is obtained as:

$$\omega \equiv \frac{\mu^2}{2\eta} \tag{2}$$

In Eq. (2), μ corresponds to the chemical potential determined as:

$$\mu = \left[\frac{\partial E}{\partial N}\right]_{v\left(\vec{r}\right)} \approx \frac{\varepsilon_{HOMO} + \varepsilon_{LUMO}}{2} \tag{3}$$

ω can be used to both note an increase in the electrophilic character of a molecular system according to its increase, and to note an increase in the nucleophilic character in relation to the decrease of ω.

The derivative of the electron density with respect to N (at constant $v\left(\vec{r}\right)$) generates a local descriptor known as Fukui function (FF) [38]:

$$f\left(\vec{r}\right) = \left[\frac{\delta\mu}{\delta v\left(\vec{r}\right)}\right]_N = \left[\frac{\partial\rho\left(\vec{r}\right)}{\partial N}\right]_{v\left(\vec{r}\right)} \tag{4}$$

For a finite difference in N, and in a frozen core approach, FF can be obtained as:

$$f^{+}\left(\vec{r}\right) = \left[\frac{\partial\rho\left(\vec{r}\right)}{\partial N}\right]^{+}_{v\left(\vec{r}\right)} \approx \rho_{LUMO}\left(\vec{r}\right) \tag{5}$$

$$f^{-}\left(\vec{r}\right) = \left[\frac{\partial\rho\left(\vec{r}\right)}{\partial N}\right]^{-}_{v\left(\vec{r}\right)} \approx \rho_{HOMO}\left(\vec{r}\right) \tag{6}$$

where $\rho_{LUMO}(\vec{r})$ and $\rho_{HOMO}(\vec{r})$ represent the LUMO and HOMO densities, respectively. In Eq. (5), $f^{+}(\vec{r})$ is the variation of the electronic density with respect to the increase in N, and it allows to identify electrophilic or selective sites to nucleophilic attacks; while, in Eq. (6), $f^{-}(\vec{r})$ is the variation of the electronic density with respect to the decrease in N, identifying nucleophilic or selective sites to electrophilic attacks. In this study, $f^{+}(\vec{r})$ and $f^{-}(\vec{r})$ will only be represented as f^{+} and f^{-} in order to simplify. Note that, FF have been connected with global properties as hardness, softness ($S=1/\eta$) and electrophilicity [34], deriving in local descriptors that contain the same information as the FF plus additional information related with the global reactivity. For example, local electrophilicity (or local philicity) can be defined as $\omega_k = \omega f_k^{+}$, where f_k^{+} is the condensed f^{+} on an atom (say k) [37, 39, 40]; the direct relation between f^{+} and ω_k is clear, then, the site with the maximum electrophilicity (the most electrophilic site) will be at the site where f^{+} is at its maximum.

Although, intramolecular reactivity and frontier-controlled interactions can be appropriately described by FF and derived local indexes because they are predominantly covalent in nature, intermolecular reactivity or charge-controlled interactions are not described adequately in all cases by FF; in this case, net charge and related properties to provide a better description of the electronic reactivity [37, 41, 42] . Taking these considerations into account, two categories of local reactivity descriptors will be used through this article, as it was usefully implemented by Fievez et al. to study the oxidation of methanol on supported vanadium oxides [42]: a) to characterize the intramolecular or frontier-controlled reactivity, FF will be used as derived in Eqs. (5) and (6); b) in order to analyze the intermolecular reactivity (non-bonding interactions, specifically), and expecting that physisorption of molecules in G systems is a charge-controlled interaction, molecular electrostatic potential (MEP) will be used for its analysis. Note that, MEP surface is useful to determine sites with negative (red color) or positive charge (blue color) excesses.

Moreover, charge on G (Q_G) was used as a charge transfer descriptor: when Q_G is positive, it indicates that G loses electronic population, while in negative value, it indicates that the functional groups or dopant atoms transfer electrons to G; charges were derived of Mulliken population analysis (MPA). Dipole moment ($\vec{p}$) was used in some cases.

Computational details

For all molecular simulations, a finite zigzag G lattice containing 16 hexagonal cells was used. For the modeling of GO, the presence of functional groups was considered according to experimental evidence: analysis by techniques as NMR [6, 7], AFM [43, 44] and STM [45] suggest that the bulk of GO is mainly functionalized with hydroxyl and epoxide groups; while, edges are functionalized with carbonyl and carboxyl groups. Considering these observations, in the basal plane of G, hydroxyl and epoxide groups were used to generate G-OH and G-O systems, respectively; on the other hand, a carboxyl and carbonyl group was formed in edges, generating the G-COOH and G-CO models, respectively. Therefore, since superficial functional groups in GO are in larger concentration with respect to edge groups, bi-functionalized models were built: G-2(OH) and G-2(O). For doped G, the following were used as dopant atoms: nitrogen (N), boron (B) and phosphorous (P); the models G-N, G-B and G-P contain a dopant atom, while G-2N, G-2B and G-2P contain two dopant atoms. All functionalized and doped graphene systems are shown in Scheme 1.

The molecular structures were optimized in a first stage by means of the semiempirical method PM6 [46], implemented in the software MOPAC2009 [47]. In this stage, for each system (described in the previous paragraph) several models were proposed to determine the most favorable sites for functionalization or doping, as well as the relative positions of functional groups in the case of bi-functionalized and bi-doped arrangements. Then, in a second stage, the most stable structures were optimized at DFT level using the functional of Perdew, Burke and Ernzerhof (PBE) [48] with the DZP basis set of Ahlrichs. In geometry optimizations and SCF steps, convergence tolerance values of $1{\cdot}10^{-6}$ and $1{\cdot}10^{-8}$ u.a. were used, respectively. Vibrational frequencies were obtained to insure that optimized molecular structures correspond to energy minimum states, obtaining positive frequencies in all cases. DFT calculations were carried out in the calculation package ORCA 2.8.0 [49]. The graphical user interface Gabedit was used for the production of surfaces [50].

Results and discussion

Table 1 shows for all G systems (pristine, functionalized and doped) the global reactivity indexes η and ω, the charge in G (Q_G), and the dipole moment (p). Figure 1 shows the electrophilic (f^{+}) and nucleophilic (f^{-}) FF calculated for pristine G; Figs. 2, 3 and 4 show the f^{+}, f^{-} and MEP surfaces, respectively, computed for functionalized and doped G systems. In the first part of the analysis, we will examine the reactivity properties of functionalized G to continue with the doped models.

In the analysis, η and ω of pristine G will be taken as reference, corresponding to 0.90 and 8.09 eV, respectively. Local descriptors, f^{+} and f^{-} (Fig. 1) show that susceptible sites to nucleophilic and electrophilic attack are located on the edge carbon atoms, in good agreement with experimental and theoretical analysis showing the inert reactivity of the basal plane of G [5, 24–26].

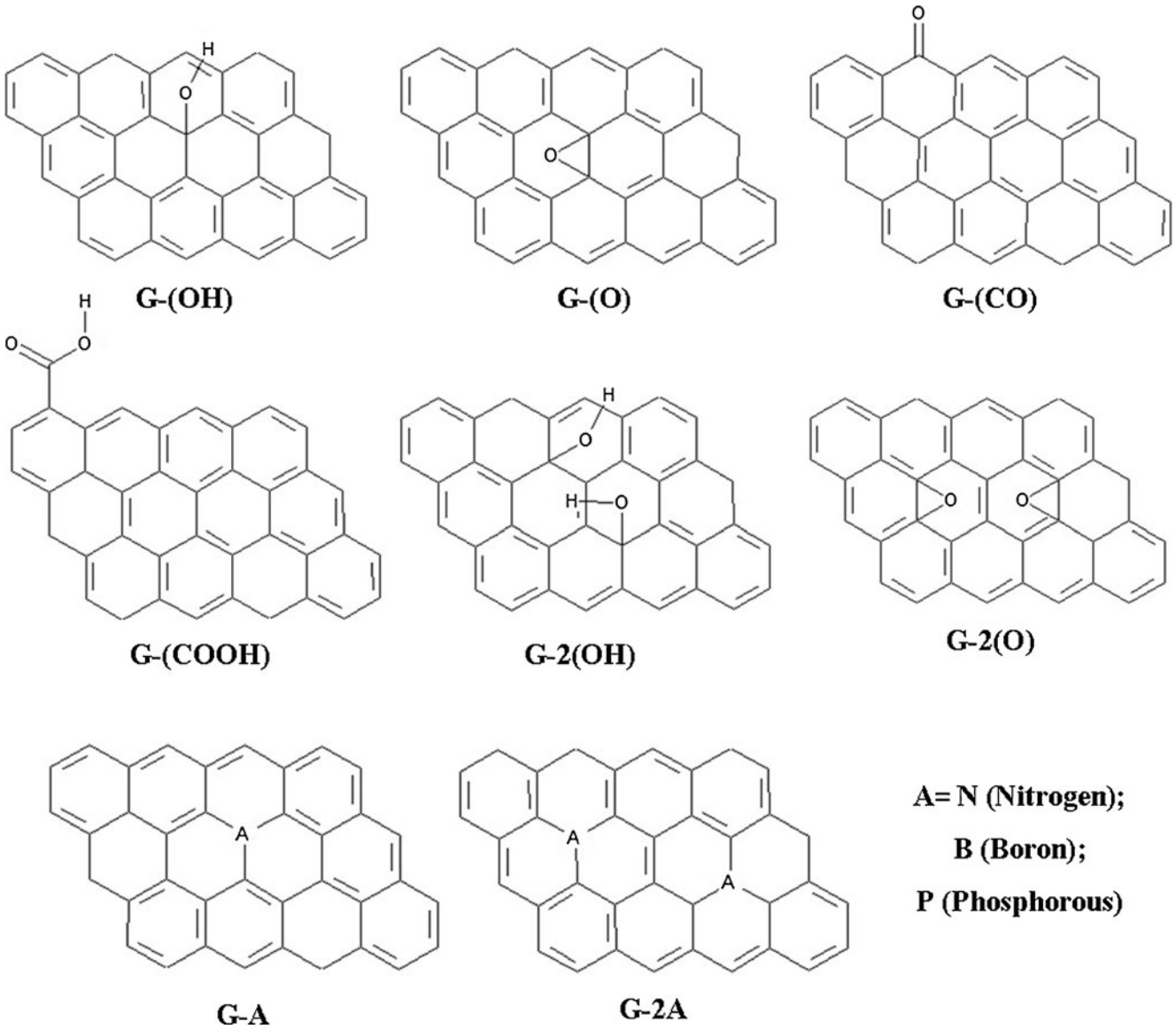

Scheme 1 Models for oxidized and doped graphene systems used in this work. Terminal hydrogens were deleted in order to simplify

Functionalized graphene with oxygen-containing functional groups

Graphene with hydroxyl groups

In the first place, the functionalization with only a hydroxyl group resulted in an insignificant change in the electronic global reactivity of G as well as in its acceptor character, keeping η and ω of pristine G. However, since superficial functional groups in GO are in a larger concentration, a G model containing two –OH was built [G-2(OH)]. In this case, it is possible to estimate in a better way the effect that the –OH groups have on G, according to the chemical intuition. Functionalization with an acceptor group causes G to lose electrical charge (0.14 electrons), increasing its electrophilic character; this produces an increase of 14.29 eV in ω; also, a decrease of 0.55 eV in η indicates an enhancing in the electronic global reactivity.

According to FF, in G-OH, susceptible sites to electrophilic attack identified by f^- are located in peripheral carbon atoms; besides, the largest electronegativity of –OH causes an increase in the donor character of carbon atoms near the functional group. Another relevant point is that the increase of the –OH groups also improves the acceptor character of basal plane of G, particularly on those carbon atoms near the functional groups, caused by electron transfer from G to the hydroxyl (0.14 electrons). Given that G loses electron population due to functionalization, the acceptor character (that it can be associated to the electrophilic reactivity) should be located at G, in good agreement with the calculated f^+. This

Table 1 Molecular hardness (η), electrophilicity (ω), charge in G (Q_G), and dipole moment (p)

System	η (eV)	ω (eV)	Q_G	p (D)
G	0.90	8.09	0.00	0.00
G-OH	0.91	8.07	0.07	1.46
G-O	0.97	7.67	0.21	1.60
G-COOH	0.84	9.51	0.07	2.54
G-CO	1.13	6.16	0.22	4.22
G-2(OH)	0.35	22.38	0.14	1.61
G-2(O)	0.91	8.22	0.50	3.54
G-N	0.35	15.57	0.61	0.84
G-B	0.89	8.84	−0.40	1.03
G-P	0.52	12.81	−0.72	1.33
G-2N	0.32	15.77	1.21	0.00
G-2B	0.20	49.14	−0.83	0.01
G-2P	0.86	8.43	−1.37	2.51

increase in the electrophilic character determined by mean of f^+ is in agreement with the increase of ω and the decrease of η for G-2(OH).

For charge-controlled intermolecular interactions, MEP shows that hydroxyl groups become more negatively-charged than G (as noted before), allowing the physisorption of electron-deficient sites in small molecules and the interaction with metal clusters [27]. On the other hand, positively-charged carbon atoms around the functional group would allow enhancement of the physisorption of molecules with negatively-charged sites as for nitrogen oxides which has been determined by DFT calculations [51]. Moreover, in a second stage, f^+ indicates that active carbon atoms in the bulk (susceptible to nucleophilic attacks) allow establishment of covalent bond with adsorbates (chemisorption), in according to, and explaining, the results of Tang and Cao [51].

Graphene with epoxide groups

With the inclusion of epoxide groups, global reactivity indexes do not change significantly with reference to pristine G: ω experiences a slight increase of −0.41 (0.13) eV in G-O (G-2(O)); while η has a negligible variation. Note that, practically null change in global reactivity is also observed from the point of view of the intramolecular local reactivity, since, f^- and f^+ computed in G-O and G-2(O) are similar to the one found for pristine G (Fig. 1).

Regarding the charge transfer processes, epoxide group gains more electric charge from G with respect to hydroxyl, 0.21 (0.50) electrons in G-O (G-2(O)), in good agreement with DFT calculations [27]; in these cases, the charge is mainly transferred from the carbon atoms linked to oxygen, decreasing the loss of charge in the other carbon atoms of G. This observation can be clarified by analyzing the dipole moment vector ($\vec{p}$) (Fig. 5) which in G-OH [G-2(OH)] is oriented in diagonal direction to basal plane, indicating a larger redistribution of the charge on the bulk; while, in G-O [G-2(O)], $\vec{p}$ is oriented in perpendicular direction to G, indicating displacement of electrons toward oxygen from carbon atoms linked to it.

On the other hand, MEP shows that oxygen atoms in epoxide groups are electron-sufficient sites, allowing intermolecular non-bonded interactions with positive centers; for example, enhancing physisorption of polar adsorbates by hydrogen bond interactions. Note that in these cases, FF do not suggest the chemisorption on the basal plane, unlike G with hydroxyl groups.

Since the functionalization with epoxide does not cause a variation in global and local reactivity indexes of basal plane of G, these results suggest that hydroxyl groups cause the increase in its chemical reactivity.

Graphene with carboxyl group

In relation to the functionalization of G with the –COOH group in the edge, regarding the pristine G a weak increase of 1.51 eV in ω can be observed, and a negligible reduction of only 0.06 eV in η. In addition, FF indicates that the most significant change to local level is observed in the carbonyl fraction of the functional group; in this case, the calculated f^+ indicates that carbonyl fraction is an electronic density acceptor, as well as the carbon atoms in the edges, contributing to the high reactivity that G edge contains [5, 24–26].

In other respects, the Q_G is 0.07, produced by electron transfer from G to carboxyl, in agreement with acceptor

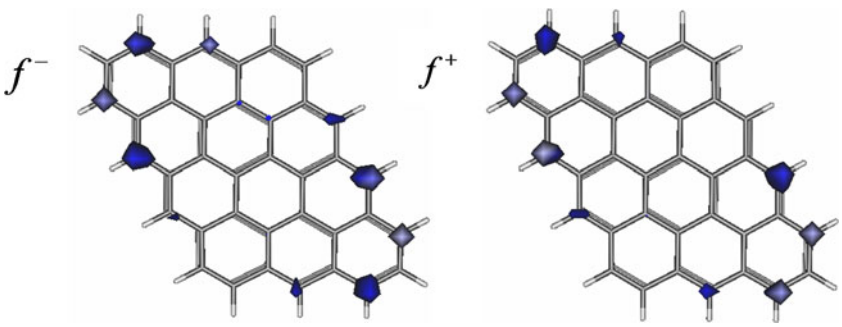

Fig. 1 Fukui functions for susceptible sites to electrophilic (f^-) and nucleophilic (f^+) attack calculated in G

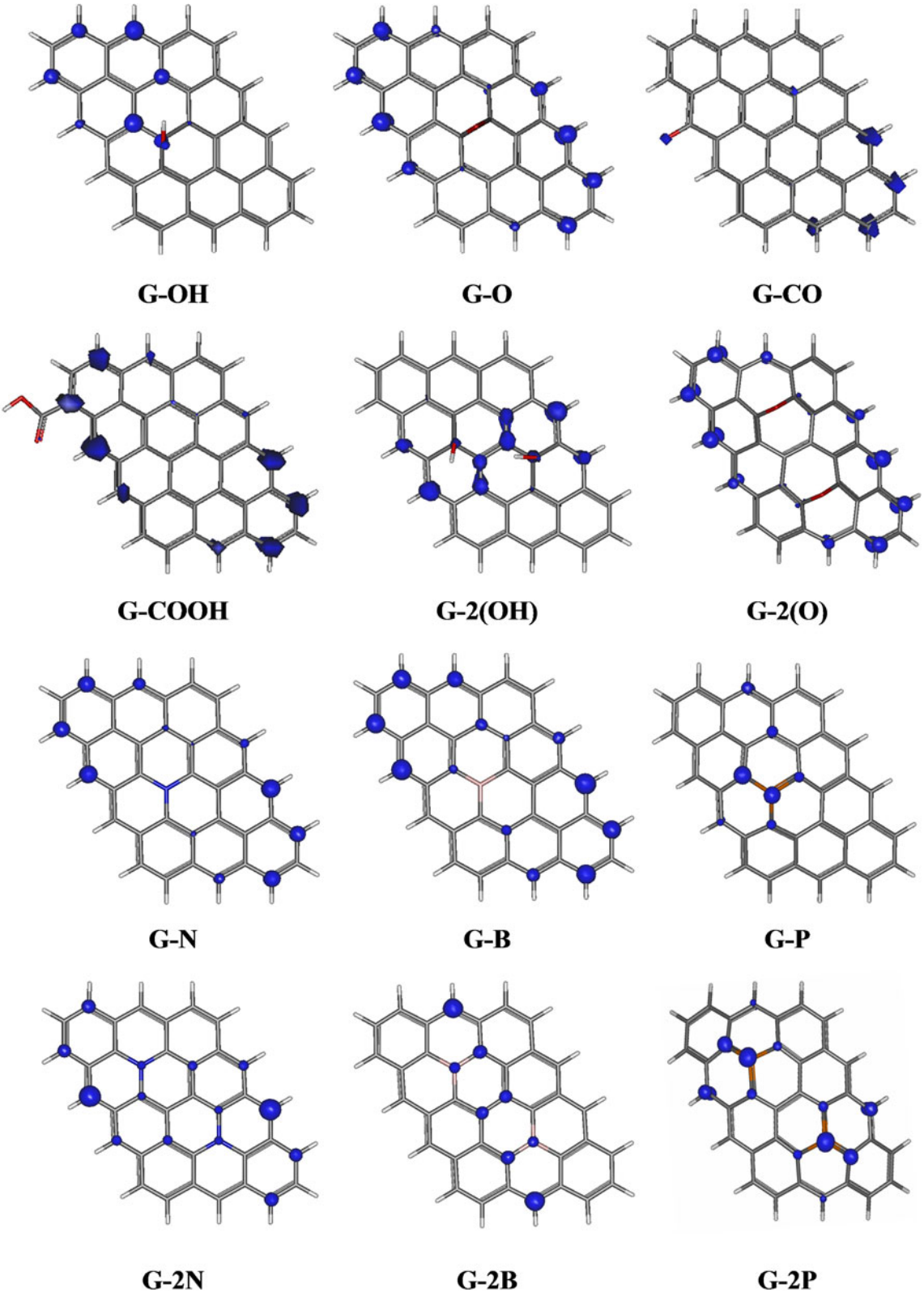

Fig. 2 Fukui function for electrophilic attack ($f^{-} \approx \rho_{HOMO}$) in G models

character that chemically characterizes to the functional group; also, this result contradicts the one found by Al-Aqtach and Vasiliev in carboxylated G [52]: in their study, they find electron transfer in direction COOH→G, however,

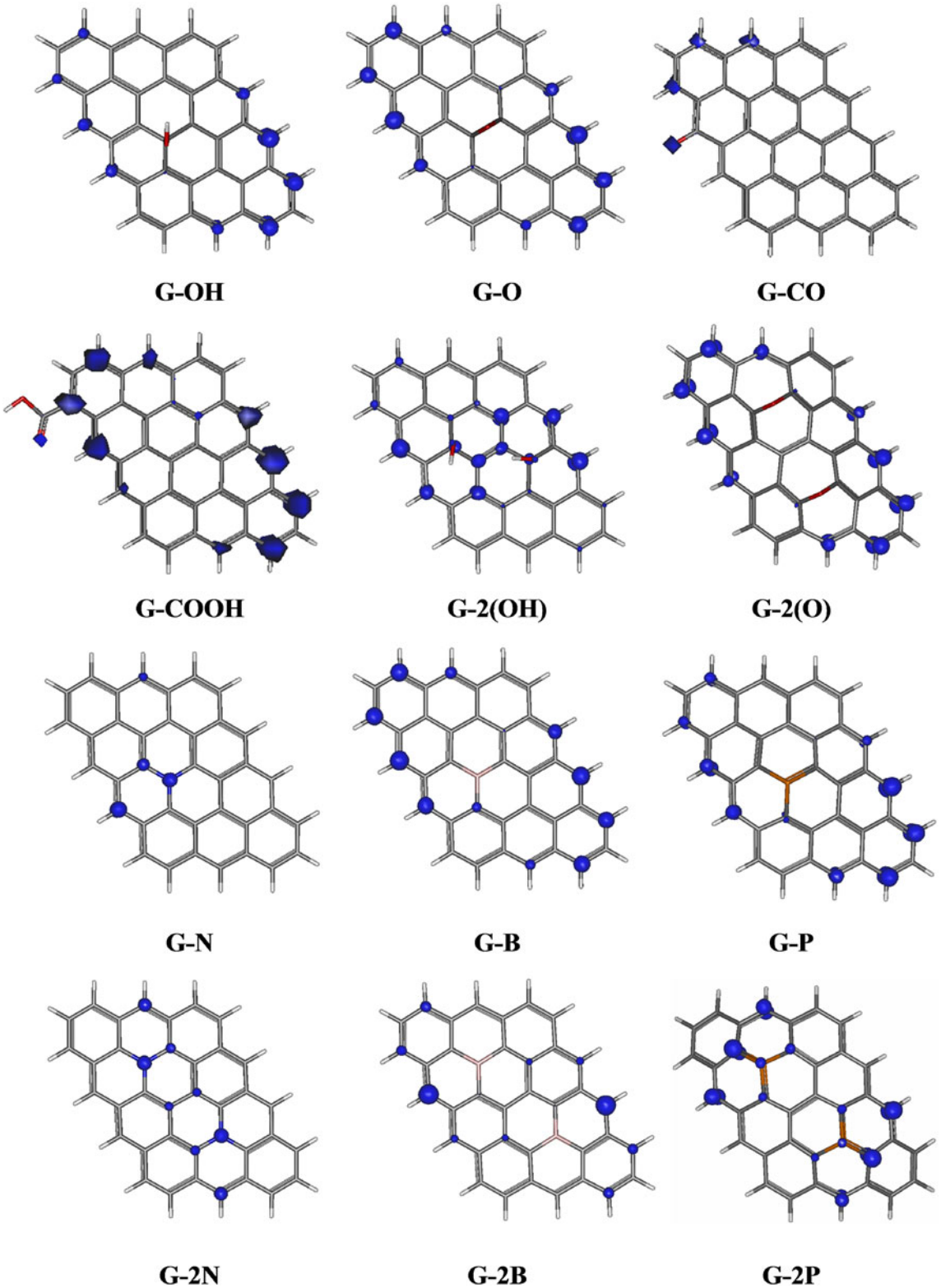

Fig. 3 Fukui function for nucleophilic attack ($f^{+}\approx\rho_{LUMO}$) in G models

the study is limited in that –COOH is adsorbed in the basal plane, whereas, the experimental evidence shows that –COOH groups are mainly functionalized in edges [6, 7], explaining the difference with the result of this work.

In this case, MEP indicates that the negatively charged carbonyl highly enhance the intermolecular interactions with the G edge. Then, carboxyl groups allow improving the physisorption of polar molecules by hydrogen bonds

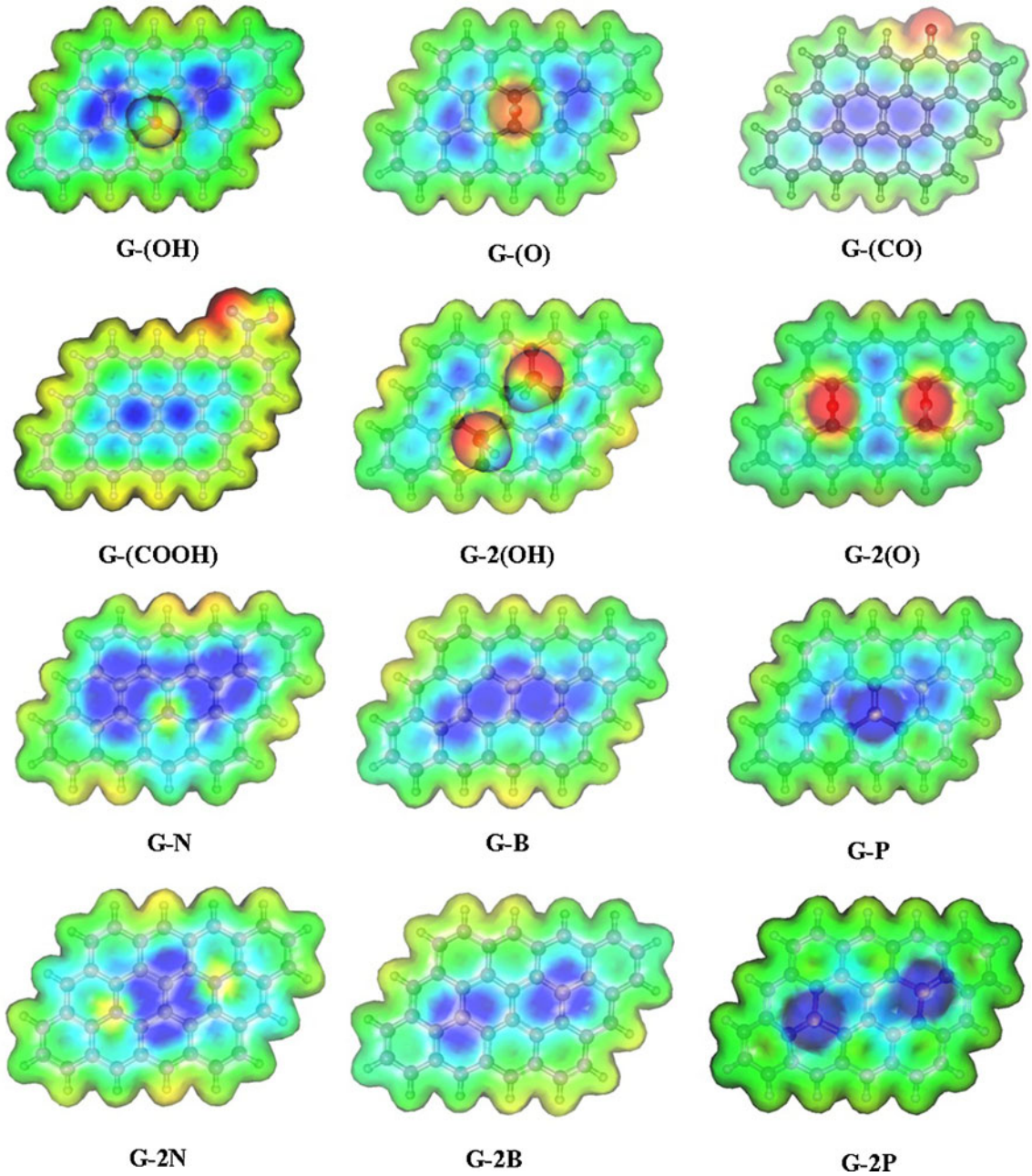

Fig. 4 Molecular electrostatic potential (MEP) surfaces for oxidized and doped graphene systems

interactions. Besides, f^+ shows that carbonyl fraction would be able to serve as the site for chemisorption of nucleophiles sites in molecules (sites that have an excess of electrons, in general), however, the negatively-charged carbonyl fraction would interpose a high barrier to the process.

Graphene with carbonyl group

Regarding the formation of a carbonyl group in G edge, it is noted that the largest electronegativity of oxygen with respect to carbon [2.55(C) versus 3.44 (O), in Pauling scale] causes that oxygen atoms to gain electronic population (0.22 electrons) inducing an important redistribution of the global charge, with a p of 4.22 D. However, the presence of a more electronegative atom does not have a significant effect on the global parameters (ω and η) with respect to pristine G. In addition, f^- and f^+ indicate that the susceptible sites to be donors or acceptors of electrons are mainly located on carbon atoms in the edges, as in pristine G. Moreover, f^- is not located on the carbon atoms adjacent to the functional group, but on the near oxygen atom, because these transfer electrons to oxygen, stopping them from behaving as

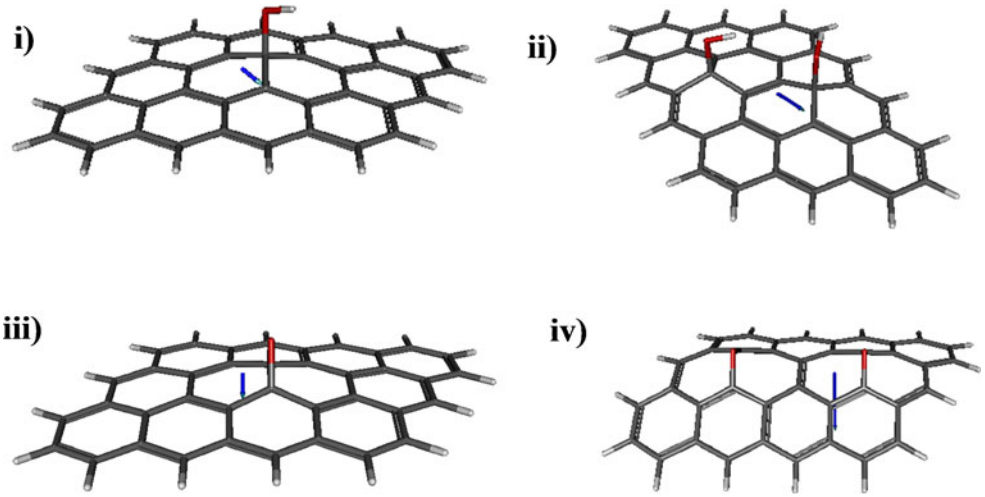

Fig. 5 Dipole moment vector ($\vec{p}$) (*blue arraw*) in: **i**) G-OH, **ii**) G-2(OH), **iii**) G-O, and **iv**) G-2(O)

donors. Besides, FF shows oxygen as a susceptible site to nucleophilic and electrophilic attacks, suggesting that it is an active site for frontier-controlled redox reactions.

For intermolecular interactions, the large electronegativity of oxygen allows it to also be an electrophilic site according to MEP, improving and serving as a site for the physisorption by hydrogen bonds of negatively polarized atoms in molecules as H_2O or NH_3[28]. As noted before, FF shows that O is an active site for frontier-controlled reactions, then, the chemisorption process would take place in this site; for example, lone-pair in O atom can establish a dative covalent bond with transition metals.

Doped graphene

N-doped graphene

Focusing in N-doped G, doping increases the electrophilic global index ω in 7.48 (7.68) eV for G-N (G-2N); besides, the absolute hardness is highly decreased in 0.55 (0.58) eV for G-N (G-2N), indicating an increase in the electronic reactivity due to doping.

In terms of the local descriptors, the susceptible sites to electrophilic attacks in G are not changed significantly for insertion of one or two N atoms, keeping f^- on peripheral carbon atoms. However, f^+ indicates that N is a susceptible site to nucleophilic attacks, according to its large electronegativity with respect to C atoms [3.04 (N) versus 2.55 (C)].

The increase in the number of N atoms also influences a charge transfer from G, also observed in N-doping studies of G and carbon nanotubes [16, 29]. In Table 1, it can be seen that Q_G in G-N (G-2N) is 0.61 (1.21), indicating a charge transfer in direction G→N. Note that, as a consequence of this charge transfer, carbon atoms near N become more positively charged and susceptible to nucleophilic attacks in agreement with f^+ located on these. The change in the local reactivity is also useful in the design or improvement of electrochemical sensors, because dopant and around carbon atoms (where the f^+ value is maximum) would be able to serve as active sites of detection by frontier-controlled redox processes. The improvement in electrochemical sensing by use of N-doped G has been successfully determined in PtRh electrodes [53] and sensing of bisphenol A, glucose, dopamine, ascorbic and uric acid [54–56].

With respect to the intermolecular interactions, by MEP it is clear to note that charge distributions in N-doped G enhance the reactivity of the G bulk. Electron-deficient carbon atoms around N improve the physisorption of small systems as has been determined for oxygen molecules in order to enhance reduction processes in fuel cells [57–61] and performance-storage in lithium-oxygen ion batteries [62]. On the other hand, as noted before, f^+ indicates that dopant and around carbon atoms would be able to serve as active sites for frontier-controlled reactions, as chemisorption of nucleophilic or donors species.

B-doped graphene

In G-B, the insertion of an atom with five electrons turns G into an electron-deficient system [23, 30–32], causing an increase in the global electrophilic character of G, being more significant with the increase in the number of dopants. This can be observed in the increase of ~41 eV in ω of G-2B with respect to pristine G, while the electronic reactivity is improved in 0.70 eV.

In addition, it is found that the minor electronegativity of B with respect to C atoms [2.04 (B) versus 2.55 (C)] causes a charge displacement in direction B→G, of 0.40 (0.83) electrons for G-B (G-2B). This causes f^- to be mainly located on B and carbon atoms adjacent to B, which act as donors. Also, f^+ shows that susceptible sites to nucleophilic attacks are mainly located in carbon atoms in the edges. As the doping with N, B atoms and carbon atoms around B with nucleophilic character

would be able to be used as a strategy to increase the electrochemical activity of G in its application to design electrochemical sensors, and be good for the storage in lithium ion batteries or fuel cells.

Respecting intermolecular reactivity, MEP shows that positively-charged B atom allows enhancement of the physisorption of anions or negatively-charged sites in molecules. For chemisorption processes, f^- indicates that C atoms around of the dopant are potential sites to bond electrophiles or acceptor species. Analyzing the MEP surface, it is not possible to find in the bulk sites with electrons excess, which does not explain the improvement in adsorption of Li^+ [21, 22, 30] and hydrogen [32], suggesting that in these cases adsorption is a frontier-controlled process; then, active sites to the chemisorption are characterized by the maximum values of f^-, as noted before. Further, on the basis of these results, the tight chemisorption of NH_3 on B-doped G [63] can be explained as a mechanism of two stages: first, in a charge-controlled step, positively-charged B atoms (see MEP) improving the interaction with polarized nitrogen atom of the NH_3 molecule; then, in a frontier-controlled step, a B-N covalent bond is formed since B atoms are susceptible sites to nucleophilic attacks according to f^-.

P-doped graphene

Unlike N and B, the doping with P does not cause an important increase of the acceptor character, even increasing the number of dopant atoms. With respect to pristine G, in G-P (G-2P), ω is larger in 4.72 (0.34) eV. On the other hand, P atoms are potential donor and acceptor sites according to f^- and f^+; this dual character would be able to explain the minor change in the global reactivity descriptors in reference to G. Moreover, f^+ shows that doping increases the electrophilic sites in the bulk, according to the one suggested by Garcia et al. [33].

Theoretically, it has been noted that the high electron population of P causes a charge transfer in direction P→G [64]. In this study, it is found that G gains 0.72 (1.37) electrons in G-P (G-2P). The decrease in the electronic population of P should increase its local electrophilic character, however, f^+ shows that P atom is a better donor than that near carbon atoms. This can be explaining by means of the decrease of electron density on P, allowing to relax the molecular structure of G-P systems.

With respect to the intermolecular reactivity, computed MEP shows that P atoms are positively charged, enhancing the physisorption of chemical species with negatively-charged centers or lone-pair electrons. Consecutively, covalent bonding with P atom (chemisorption) is possible because it is a susceptible site to nucleophilic attacks according to computed f^+. This observation is in good agreement with the chemisorption of O_2 on P-doped G determined at theoretical level by Dai and Yuan [64]. It is worth noting that f^- suggests that P atom would also serve as a site for the chemisorption of electrophiles species (acceptors), however, the positive charge on P could avoid the physisorption toward the site. Finally, FF show that near C atoms of dopant would also be able to serve as sites for chemisorption of adsorbates.

Conclusions

In summary, on the basis of the conceptual formulation of DFT, MPA and MEP analysis, this study contributes to understanding the changes in the local and global electronic reactivity of oxidized and doped G systems.

Results show that electronic reactivity of G is due mainly to the C atoms in edges, in agreement with experimental and theoretical observations. In GO, the global and intramolecular local reactivity of the basal plane is improved mainly by hydroxyl groups. For charge-controlled intermolecular interactions, hydroxyl groups allow the physisorption of small molecules, while, active carbon atoms around functional group would allow enhancement of the consecutively chemisorption. On the other hand, negatively-charged epoxide, carbonyl and carboxyl groups allow enhancement of intermolecular non-bonded and hydrogen bond interactions with positive centers.

On the other hand, doping with N and B atoms increases the electrophilic character and the intramolecular reactivity in the bulk. Regarding N-doping, calculations show that N and around carbon atoms (susceptible sites to nucleophilic attacks) would be able to serve as active sites of detection by frontier-controlled redox processes, explaining the improvement in electrochemical sensing; in addition, electron-deficient carbon atoms around N improve the physisorption. With respect to B-doped G, dopant and carbon atoms adjacent to B act as donor sites, suggesting that adsorption of Li^+ and hydrogen on B-doped G is a frontier-controlled process, since it is not possible to find in the bulk sites with electron excess. Moreover, positively-charged B atoms improve the intermolecular interaction with polarized molecules such as NH_3; consecutively, in a frontier-controlled step, chemisorption is possible. Finally, doping with P increases the electrophilic reactivity in the bulk. Also, P atoms enhance the physisorption of chemical species with negatively-charged centers or lone-pair electrons, and consecutively chemisorption on P is possible.

Acknowledgments The author thanks Juan M. Perez for the provided help in the last stage of the article, and to reviewers for comments and suggestions.

References

1. Bolotin KI, Sikes KJ, Jiang Z, Klima M, Fudenberg G, Hone J, Kim P, Stormer HL (2008) Ultrahigh electron mobility in suspended graphene. Solid State Commun 146(9–10):351–355
2. Geim AK, Novoselov KS (2007) The rise of graphene. Nat Mater 6(3):183–191
3. Chen S, Wu Q, Mishra C, Kang J, Zhang H, Cho K, Cai W, Balandin AA, Ruoff RS (2012) Thermal conductivity of isotopically modified graphene. Nat Mater 11:203–217
4. Lee C, Wei X, Kysar JW, Hone J (2008) Measurement of the elastic properties and intrinsic strength of monolayer graphene. Science 321(5887):385–388
5. Sharma R, Baik JH, Perera CJ, Strano MS (2010) Anomalously large reactivity of single graphene layers and edges toward electron transfer chemistries. Nano Letters 10(2):398–405
6. Lerf A, He H, Forster M, Klinowski J (1998) Structure of graphite oxide revisited. J Phys Chem B 102(23):4477–4482
7. Cai W, Piner RD, Stadermann FJ, Park S, Shaibat MA, Ishii Y, Yang D, Velamakanni A, An SJ, Stoller M, An J, Chen D, Ruoff RS (2008) Synthesis and solid-state NMR structural characterization of 13C-labeled graphite oxide. Science 321(5897):1815–1817
8. Hummers WS, Offeman RE (1958) Preparation of graphitic oxide. J Am Chem Soc 80(6):1339–1339
9. Chunder A, Pal T, Khondaker SI, Zhai L (2010) Reduced graphene oxide/copper phthalocyanine composite and its optoelectrical properties. J Phys Chem C 114(35):15129–15135
10. Zhu J, Li Y, Chen Y, Wang J, Zhang B, Zhang J, Blau WJ (2011) Graphene oxide covalently functionalized with zinc phthalocyanine for broadband optical limiting. Carbon 49 (6):1900–1905
11. Pyun J (2011) Graphene oxide as catalyst: application of carbon materials beyond nanotechnology. Angew Chem Int Ed 50(1):46–48
12. Ji Z, Shen X, Zhu G, Zhou H, Yuan A (2012) Reduced graphene oxide/nickel nanocomposites: facile synthesis, magnetic and catalytic properties. J Mater Chem 22(8):3471–3477
13. Zhang N, Qiu H, Liu Y, Wang W, Li Y, Wang X, Gao J (2011) Fabrication of gold nanoparticle/graphene oxide nanocomposites and their excellent catalytic performance. J Mater Chem 21 (30):11080–11083
14. Wei Y, Gao C, Meng F-L, Li H-H, Wang L, Liu J-H, Huang X-J (2011) SnO2/Reduced graphene oxide nanocomposite for the simultaneous electrochemical detection of cadmium(II), lead(II), copper(II), and Mercury(II): an interesting favorable mutual interference. J Phys Chem C 116(1):1034–1041
15. Qian Z, Shaojun Y, Jing Z, Ling Z, Pingli K, Jinghong L, Jingwei X, Hua Z, Xi-Ming S (2011) Fabrication of an electrochemical platform based on the self-assembly of graphene oxide–multiwall carbon nanotube nanocomposite and horseradish peroxidase: direct electrochemistry and electrocatalysis. Nanotechnology 22 (49):494010
16. Geng D, Yang S, Zhang Y, Yang J, Liu J, Li R, Sham T-K, Sun X, Ye S, Knights S (2011) Nitrogen doping effects on the structure of graphene. Appl Surf Sci 257(21):9193–9198
17. Denis PA (2011) Chemical reactivity of lithium doped monolayer and bilayer graphene. J Phys Chem C 115(27):13392–13398
18. Dai J, Yuan J, Giannozzi P (2009) Gas adsorption on graphene doped with B, N, Al, and S: a theoretical study. Appl Phys Lett 95 (23):232105
19. Cazorla C (2010) Ab initio study of the binding of collagen amino acids to graphene and A-doped (A=H, Ca) graphene. Thin Solid Films 518(23):6951–6961
20. Mousavi H, Moradian R (2011) Nitrogen and boron doping effects on the electrical conductivity of graphene and nanotube. Solid State Sci 13(8):1459–1464
21. Gao S, Ren Z, Wan L, Zheng J, Guo P, Zhou Y (2011) Density functional theory prediction for diffusion of lithium on boron-doped graphene surface. Appl Surf Sci 257(17):7443–7446
22. Wu Z-S, Ren W, Xu L, Li F, Cheng H-M (2011) Doped graphene sheets as anode materials with superhigh rate and large capacity for lithium ion batteries. ACS Nano 5(7):5463–5471
23. Zhou YG, Zu XT, Gao F, Nie JL, Xiao HY (2009) Adsorption of hydrogen on boron-doped graphene: a first-principles prediction. J Appl Phys 105(1):014309
24. Hernández Rosas J, Ramírez Gutiérrez R, Escobedo-Morales A, Chigo Anota E (2011) First principles calculations of the electronic and chemical properties of graphene, graphane, and graphene oxide. J Mol Model 17(5):1133–1139
25. Peralta-Inga Z, Murray JS, Edward Grice M, Boyd S, O'Connor CJ, Politzer P (2001) Computational characterization of surfaces of model graphene systems. J Mol Struct (THEOCHEM) 549(1–2):147–158
26. Radovic LR (2009) Active sites in graphene and the mechanism of CO2 formation in carbon oxidation. J Am Chem Soc 131 (47):17166–17175
27. Acharya CK, Sullivan DI, Turner CH (2008) Characterizing the interaction of Pt and PtRu clusters with boron-doped, nitrogen-doped, and activated carbon: density functional theory calculations and parameterization. J Phys Chem C 112(35):13607–13622
28. Berashevich J, Chakraborty T (2010) Doping graphene by adsorption of polar molecules at the oxidized zigzag edges. Phys Rev B 81(20):205431
29. Gong K, Du F, Xia Z, Durstock M, Dai L (2009) Nitrogen-doped carbon nanotube arrays with high electrocatalytic activity for oxygen reduction. Science 323(5915):760–764
30. Wang X, Zeng Z, Ahn H, Wang G (2009) First-principles study on the enhancement of lithium storage capacity in boron doped graphene. Appl Phys Lett 95(18):183103
31. Panchakarla LS, Subrahmanyam KS, Saha SK, Govindaraj A, Krishnamurthy HR, Waghmare UV, Rao CNR (2009) Synthesis, structure, and properties of boron- and nitrogen-doped graphene. Adv Mater 21(46):4726–4730
32. Beheshti E, Nojeh A, Servati P (2011) A first-principles study of calcium-decorated, boron-doped graphene for high capacity hydrogen storage. Carbon 49(5):1561–1567
33. Baltazar SE, García ALE, Pérez-Robles JF, Romero AH, Rubio Secades Á (2008) Influence of S and P doping in a graphene sheet. J Comput Theor Nanosci 5:1–9
34. Geerlings P, De Proft F, Langenaeker W (2003) Conceptual density functional theory. Chem Rev 103(5):1793–1874
35. Parr RG, Pearson RG (1983) Absolute hardness: companion parameter to absolute electronegativity. J Am Chem Soc 105 (26):7512–7516
36. Parr RG, Lv S, Liu S (1999) Electrophilicity index. J Am Chem Soc 121(9):1922–1924
37. Chattaraj PK, Sarkar U, Roy DR (2006) Electrophilicity Index. Chem Rev 106(6):2065–2091
38. Parr RG, Yang W (1984) Density functional approach to the frontier-electron theory of chemical reactivity. J Am Chem Soc 106(14):4049–4050
39. Pérez P, Toro-Labbé A, Aizman A, Contreras R (2002) Comparison between experimental and theoretical scales of electrophilicity in benzhydryl cations. J Org Chem 67(14):4747–4752
40. Chattaraj PK, Maiti B, Sarkar U (2003) Philicity: a unified treatment of chemical reactivity and selectivity. J Phys Chem A 107 (25):4973–4975
41. Chattaraj PK (2000) Chemical reactivity and selectivity: local HSAB principle versus frontier orbital theory. J Phys Chem A 105(2):511–513

42. Fievez T, Weckhuysen BM, Geerlings P, Proft FD (2009) Chemical reactivity indices as a tool for understanding the support-effect in supported metal oxide catalysts. J Phys Chem C 113(46):19905–19912
43. Cote LJ, Kim F, Huang J (2008) Langmuir−Blodgett assembly of graphite oxide single layers. J Am Chem Soc 131(3):1043–1049
44. Schniepp HC, Li J-L, McAllister MJ, Sai H, Herrera-Alonso M, Adamson DH, Prud'homme RK, Car R, Saville DA, Aksay IA (2006) Functionalized single graphene sheets derived from splitting graphite oxide. J Phys Chem B 110 (17):8535–8539
45. Pandey D, Reifenberger R, Piner R (2008) Scanning probe microscopy study of exfoliated oxidized graphene sheets. Surf Sci 602 (9):1607–1613
46. Stewart JP (2007) Optimization of parameters for semiempirical methods V: modification of NDDO approximations and application to 70 elements. J Mol Model 13(12):1173–1213
47. MOPAC2009, James J. P. Stewart, Stewart Computational Chemistry, Version 11.038W web: http://OpenMOPAC.net
48. Perdew JP, Burke K, Ernzerhof M (1997) Generalized gradient approximation made simple [Phys Rev Lett 77, 3865 (1996)]. Phys Rev Lett 78(7):1396–1396
49. Neese F (2004) ORCA—an ab initio, Density Functional and Semiempirical program package, Version 2.8. Max-Planck-Insitut für Bioanorganische Chemie, Mülheim and der Ruhr
50. Allouche A-R (2011) Gabedit—a graphical user interface for computational chemistry softwares. J Comput Chem 32(1):174–182
51. Tang S, Cao Z (2011) Adsorption of nitrogen oxides on graphene and graphene oxides: insights from density functional calculations. J Chem Phys 134(4):044710
52. Al-Aqtash N, Vasiliev I (2011) Ab initio study of boron- and nitrogen-doped graphene and carbon nanotubes functionalized with carboxyl groups. J Phys Chem C 115(38):18500–18510
53. Wang D-W, Gentle IR, Lu GQ (2010) Enhanced electrochemical sensitivity of PtRh electrodes coated with nitrogen-doped graphene. Electrochem Commun 12(10):1423–1427
54. Fan H, Li Y, Wu D, Ma H, Mao K, Fan D, Du B, Li H, Wei Q (2012) Electrochemical bisphenol A sensor based on N-doped graphene sheets. Anal Chim Acta 711:24–28
55. Wang Y, Shao Y, Matson DW, Li J, Lin Y (2010) Nitrogen-doped graphene and its application in electrochemical biosensing. ACS Nano 4(4):1790–1798
56. Sheng Z-H, Zheng X-Q, Xu J-Y, Bao W-J, Wang F-B, Xia X-H (2012) Electrochemical sensor based on nitrogen doped graphene: simultaneous determination of ascorbic acid, dopamine and uric acid. Biosens Bioelectron 34(1):125–131
57. Okamoto Y (2009) First-principles molecular dynamics simulation of O2 reduction on nitrogen-doped carbon. Appl Surf Sci 256 (1):335–341
58. Qu L, Liu Y, Baek J-B, Dai L (2010) Nitrogen-doped graphene as efficient metal-free electrocatalyst for oxygen reduction in fuel cells. ACS Nano 4(3):1321–1326
59. Yu L, Pan X, Cao X, Hu P, Bao X (2011) Oxygen reduction reaction mechanism on nitrogen-doped graphene: a density functional theory study. J Catal 282(1):183–190
60. Zhang L, Xia Z (2011) Mechanisms of oxygen reduction reaction on nitrogen-doped graphene for fuel cells. J Phys Chem C 115 (22):11170–11176
61. Zhang L, Niu J, Dai L, Xia Z (2012) Effect of microstructure of nitrogen-doped graphene on oxygen reduction activity in fuel cells. Langmuir 28(19):7542–7550
62. Li Y, Wang J, Li X, Geng D, Banis MN, Li R, Sun X (2012) Nitrogen-doped graphene nanosheets as cathode materials with excellent electrocatalytic activity for high capacity lithium-oxygen batteries. Electrochem Commun 18:12–15
63. Zhang YH, Chen YB, Zhou KG, Liu CH, Zeng J, Zhang HL, Peng Y (2009) Improving gas sensing properties of graphene by introducing dopants and defects: a first-principles study. Nanotechnology 20(18):185504
64. Dai J, Yuan J (2010) Adsorption of molecular oxygen on doped graphene: atomic, electronic, and magnetic properties. Phys Rev B 81(16):165414